

SPECTROSCOPIC APPLICATIONS OF THE  $(p, \pi^-)$  REACTION

Z.-J. Cao<sup>†</sup>, R.D. Bent, H. Nann, and T.E. Ward<sup>§</sup>  
 Indiana University Cyclotron Facility, Bloomington, Indiana 47405

Utilizing the strong selectivity of the  $A(p, \pi^-)A+1$  reaction for population of high-spin, two-particle one-hole final states, which has been observed for a number of targets in the C, Ca, and Zr mass regions<sup>1,2</sup> and two targets in the sd-shell,<sup>3</sup> we have located and identified several candidates for high-spin states in the sd-shell nuclei  $^{20}\text{Na}$ ,  $^{24}\text{Al}$ ,  $^{26}\text{Si}$ ,  $^{28}\text{P}$ ,  $^{30}\text{S}$  and  $^{31}\text{S}$ . The spin assignments are based on both the strong population of the states and the stretched-state signature of the analyzing power angular distributions.

The experiments were performed with 199.6 MeV polarized proton beams having an energy spread of about 200 keV at a beam intensity of 200 nA. Pions were detected using the QQSP spectrometer with the standard focal-plane detector array for pions.

Pion spectra corresponding to excitation energies of the residual nuclei from zero up to about 20 MeV are shown in Fig. 1. These spectra were all taken at a laboratory angle of  $30^\circ$  and a bombarding energy of 199.6 MeV, without changing the QQSP magnetic field to facilitate accurate cross energy calibrations. The  $^7\text{Li}(p, \pi^-)^8\text{B}$  (0.78 MeV) and  $^{29}\text{Si}(p, \pi^-)^{30}\text{S}$  (g.s.) peaks were used as energy calibration points in the high and low energy regions, respectively. Angular distributions of the differential cross sections and analyzing powers for several of the strongest transitions for the  $^{19}\text{F}$  and  $^{27}\text{Al}$  targets are presented in Figs. 2-4. These contain useful spectroscopic information and will be discussed below.

Four strong peaks are observed in the  $^{19}\text{F}(p, \pi^-)^{20}\text{Na}$  spectrum shown in Fig. 1(b), corresponding to excited states of  $^{20}\text{Na}$  at 0.74, 1.85,

3.01, and 4.11 MeV. We see no ground-state ( $2^+$ ) transition, probably due to the low spin of this state. All four peaks are broader than the instrumental resolution, indicating that more than one state contributes to each peak. There are several levels in  $^{20}\text{Na}$  around 0.77 MeV with  $J^\pi \leq 4^+$ . Levels of known energy but unknown spin are at 1.92 MeV, 2.89 MeV, and 4.33 MeV. Several levels with  $J \leq 5$  are known around 1.92 MeV in the isobaric analogue nucleus  $^{20}\text{F}$ .

The strong populations and analyzing power patterns can be used to make tentative spin assignments to certain levels in  $^{20}\text{Na}$ . The transitions can be grouped into two categories according to distinctly different patterns of the analyzing power angular distributions. The first group includes transitions to the 0.74 and 1.85 MeV states. The shapes of their analyzing power angular distributions, as shown in Fig. 2, are similar to those observed by Thrope<sup>4</sup> for transitions to low-spin final states. The second group includes transitions to the 3.01 and 4.11 MeV states. Their analyzing power angular distributions, as shown in Fig. 3, are similar to those observed for transitions to stretched two-particle one-hole states in near-threshold  $(p, \pi^-)$  studies on several targets from  $A = 19$  to  $A = 89$ .<sup>3,4</sup> This type of analyzing power angular distribution seems to be a "signature" of  $(p, \pi^-)$  transitions to stretched two-particle one-hole final states, and is distinctly different from the type illustrated by Fig. 2. The possible final-state spins resulting from a stretched  $2p-1h$  configuration with respect to the target nucleus,  $[(\pi d_{5/2})^2_4 (\nu d_{5/2})^{-1}]_{13/2^+}$  or  $\{[(\pi d_{5/2})(\pi d_{3/2})]_4 (\nu d_{5/2})^{-1}\}_{13/2^+}$ ,

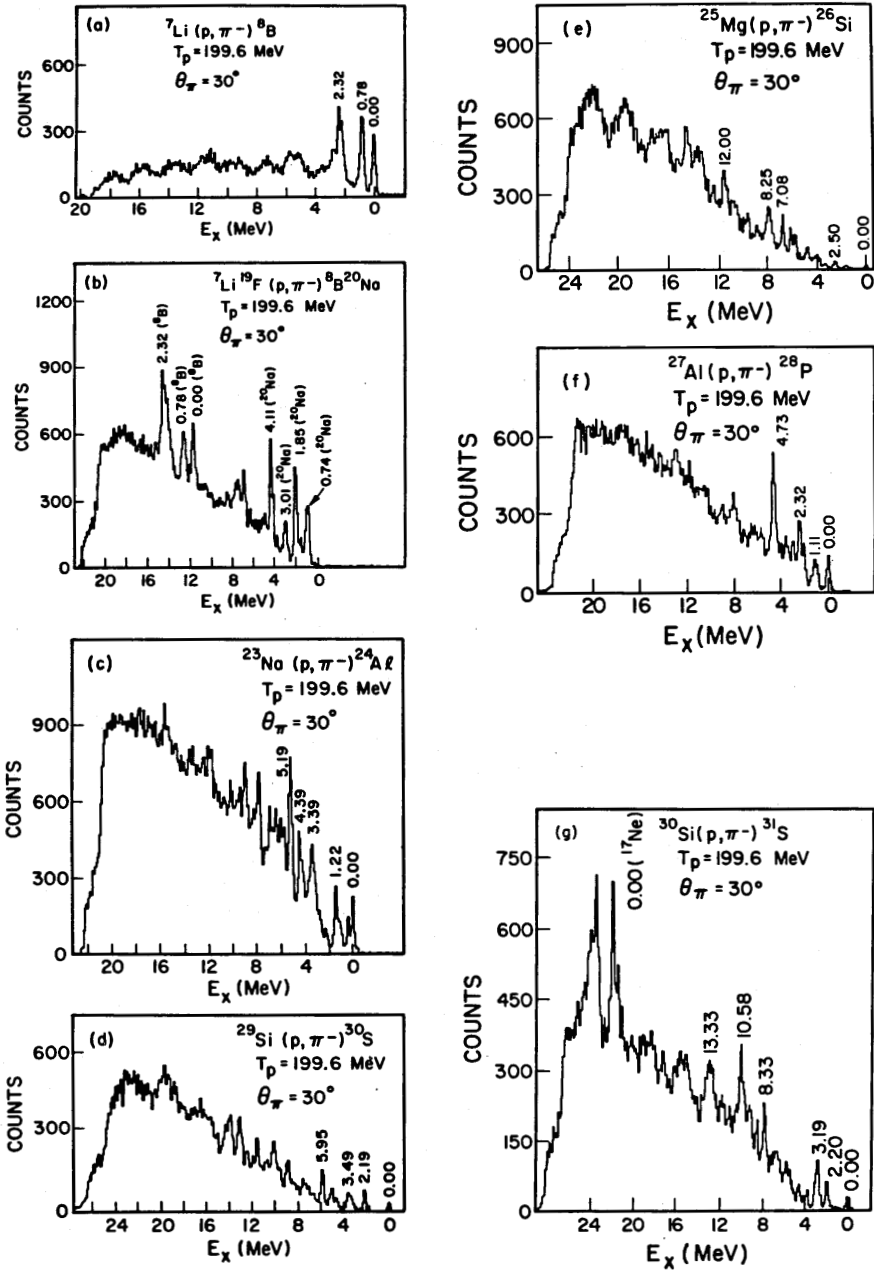


Figure 1. Spectra from the reactions  ${}^7\text{Li}(p, \pi^-){}^8\text{B}$  (a),  ${}^7\text{Li}{}^{19}\text{F}(p, \pi^-){}^8\text{B}{}^{20}\text{Na}$  (b),  ${}^{23}\text{Na}(p, \pi^-){}^{24}\text{Al}$  (c),  ${}^{29}\text{Si}(p, \pi^-){}^{30}\text{S}$  (d),  ${}^{25}\text{Mg}(p, \pi^-){}^{26}\text{Si}$  (e),  ${}^{27}\text{Al}(p, \pi^-){}^{28}\text{P}$  (f), and  ${}^{30}\text{Si}(p, \pi^-){}^{31}\text{Si}$  (g) at  $T_p = 199.6$  MeV and  $\theta_\pi = 30^\circ$ . The strong peaks seen in the high excitation energy region in Fig. 1(g) are due to oxygen in the target.

coupled to the  $1/2^+$  target ground state, are  $J^\pi = 6^+$  and  $7^+$ , assuming that all active nucleons are restricted to the sd-shell, which is reasonable for low lying excited states. Consequently, the 0.74 and 1.85

MeV states have  $J < 5$ . This agrees with existing knowledge of the level structure of  ${}^{20}\text{Na}$  and the shell model calculations of Wildenthal<sup>5</sup>, which predict a  $5^+$  level at 1.74 MeV but no higher spin levels in this

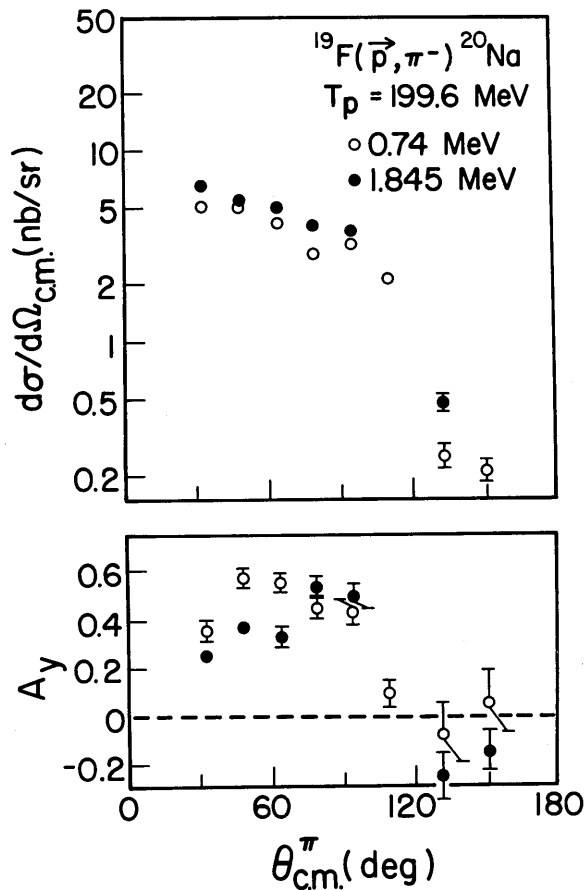


Figure 2. Comparison of the angular distributions of the cross sections and analyzing powers for transitions to the 0.74 MeV and 1.85 MeV states in the  $^{19}\text{F}(p, \pi^-)^{20}\text{Na}$  reaction at 199.6 MeV bombarding energy, showing a striking similarity between the distributions.

excitation region. The 3.01 and 4.11 MeV states may be assigned  $J^\pi = 6^+$  or  $7^+$ , based on the above analyzing power signature argument. These may correspond to the lowest  $6^+$  and  $7^+$  states predicted by Wildenthal<sup>5</sup> at 4.52 and 4.46 MeV, respectively. The spins of these states are not known from other experiments. A high-spin assignment explains why a strong 4.11 MeV peak is seen in the spectrum in a region where the  $^{20}\text{Na}$  level density is high.

Figure 1(c) shows the  $^{23}\text{Na}(p, \pi^-)^{24}\text{Al}$  spectrum. The peak at 1.22 MeV excitation energy is broader than the experimental resolution, indicating more than one contributing state. Two states are known around 1.22

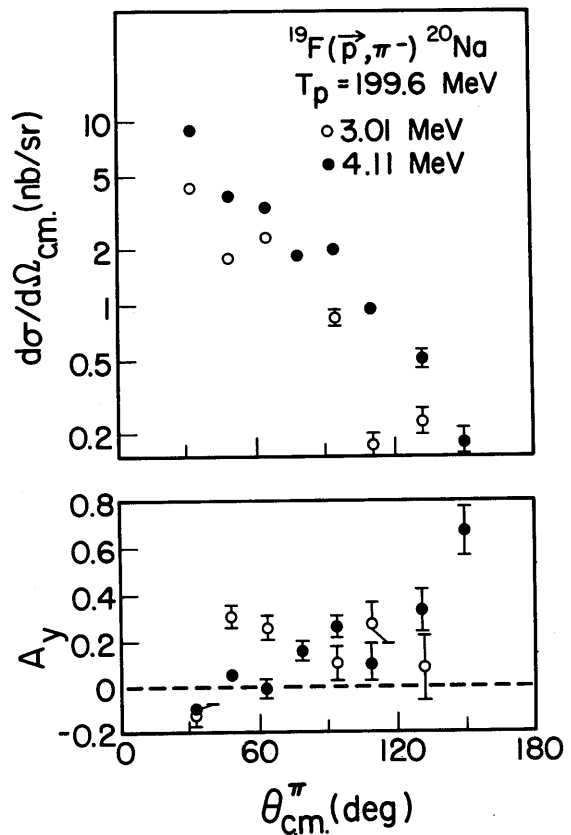


Figure 3. Comparison of the angular distributions of the cross sections and analyzing powers for transitions to the 3.01 MeV and 4.11 MeV states in the  $^{19}\text{F}(p, \pi^-)^{20}\text{Na}$  reaction at 199.6 MeV, showing some similarity between these distributions.

MeV, one at 1.12 MeV and another at 1.29 MeV, which cannot be resolved completely in our experiment. The 3.39 and 4.39 MeV peaks may also represent unresolved states. The strongest peak in the spectrum corresponds to an excitation energy of 5.19 MeV. There is no known level in  $^{24}\text{Al}$  at this excitation energy, but a number of levels are known around this energy in the isobaric analogue nucleus  $^{24}\text{Na}$ . The strong population of the 5.19 MeV state in the  $(p, \pi^-)$  reaction implies a possible two-particle one-hole high-spin [ $3 < J < 8$ ] configuration,  $[(\pi d_{5/2})^2_4 (v d_{5/2})^{-1}]_{13/2^+} \times 3/2^+$ ,  $\{[(\pi d_{5/2})(\pi d_{3/2})]_4 (v d_{5/2})^{-1}\}_{13/2^+} \times 3/2^+$ , or  $[(\pi d_{3/2})^2_2 (v d_{5/2})^{-1}]_{9/2^+} \times 3/2^+$ , for this state. This may correspond to the second  $6^+$  and/or first  $7^+$  state(s) predicted<sup>5</sup> at 5.29 and 5.31 MeV, respectively.

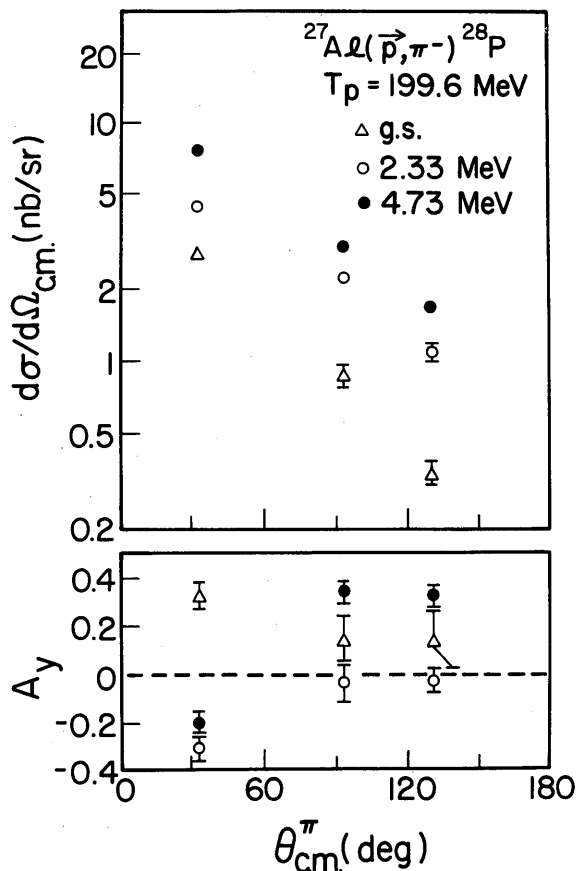


Figure 4. The angular distributions of the cross sections and analyzing powers for the ground, 2.33 MeV, and 4.73 MeV state transitions in the  $^{27}\text{Al}(p, \pi^-)^{28}\text{P}$  reaction at a bombarding energy of 199.6 MeV.

The first  $8^+$  state is predicted<sup>5</sup> at 8.29 MeV. This may correspond to one of the prominent peaks observed in the  $(p, \pi^-)$  spectrum at 7.65 and 8.90 MeV; however, a number of high spin [ $J = 7, 8$ ] states are predicted<sup>5</sup> in this energy region.

The  $^{29}\text{Si}(p, \pi^-)^{30}\text{S}$  spectrum is shown in Fig. 1(d). The ground state of  $^{30}\text{S}$  ( $0^+$ ) is weakly populated but well separated from the first excited state, so it was used as a calibration point in the low energy region, as described above. The strongest three peaks in the low energy region correspond to excitation energies of 2.19, 3.49, and 5.95 MeV. These agree with known energy

levels. The 5.95 MeV peak may correspond to the 5.90 MeV state identified from the  $(p, t)$  two-nucleon pick-up reaction at 40 MeV;<sup>6</sup> a 5.95 MeV state ( $4^+$ ) is known in the isobaric analogue nucleus  $^{30}\text{Si}$ . Peaks in the  $(p, \pi^-)$  spectrum are observed at higher excitation energies of 7.46, 9.13, 10.07, 11.53, and 13.28 MeV. The possible spin values resulting from the stretched two-particle one-hole configuration  $[(d_{3/2})^2(d_{5/2})^{-1}]_{9/2^+}$  coupled to the  $1/2^+$  target ground state are  $J^\pi = 4^+$  and  $5^+$ . Wildenthal<sup>5</sup> predicts a  $4^+$  state at 5.91 MeV, which may correspond to the strong 5.95 MeV peak in the  $(p, \pi^-)$  spectrum. The lowest lying  $5^+$  states are predicted<sup>5</sup> at 7.24, 8.94, and 10.0 MeV, in close agreement with the 7.46, 9.13, and 10.07 MeV peaks in the  $(p, \pi^-)$  spectrum.

There are no striking peaks in the  $^{25}\text{Mg}(p, \pi^-)^{26}\text{Si}$  spectrum shown in Fig. 1(e). The low lying states are weakly populated. The 7.08 MeV peak may correspond to a known state at 7.15 MeV. Two sharp peaks at 8.25 and 12.0 MeV excitation energies, where the level density is high, are candidates for high-spin [ $2 < J < 8$ ] states resulting from the stretched 2p-1h configurations  $\{[(\pi d_{5/2})(\pi d_{3/2})]_4(\nu d_{5/2})^{-1}\}_{13/2^+}$  or  $\{[(\pi d_{3/2})^2(\nu d_{5/2})^{-1}]_{9/2^+}$  coupled to the  $5/2^+$  target ground state. These may correspond to the lowest energy  $5^+$ ,  $6^+$ , and  $8^+$  states predicted by Wildenthal<sup>5</sup> at 7.04, 8.19, and 11.77 MeV, respectively.

The  $^{27}\text{Al}(p, \pi^-)^{28}\text{P}$  reaction is expected to populate most strongly high-spin final states consisting of a stretched 2p-1h configuration  $\{[(\pi d_{3/2})^2(\nu d_{5/2})^{-1}]_{9/2^+}$  coupled to the  $5/2^+$  target ground state, giving  $2 < J_f < 7$ . The strongest peak in the spectrum shown in Fig. 1 (f) occurs at  $E_x = 4.73$  MeV. The angular distribution of the analyzing power for the transition to this state shown in Fig. 4 does indeed follow the systematic pattern observed<sup>3,4</sup> for transitions to

stretched 2p-1h final states. This pattern is quite different from that observed<sup>4</sup> for transitions to low-spin final states, such as the ground state ( $3^+$ ) transition shown in Fig. 4. The angular distribution of the analyzing power for the transition to the 2.33 MeV state is similar to that for the 4.73 MeV state suggesting a stretched 2p-1h configuration for this state also. Based on the above evidence, we tentatively associate the 4.73 MeV peak in the  $(p, \pi^-)$  spectrum with the 4.53 MeV ( $6^+$ ) or 4.77 MeV ( $5^+$ ) states predicted by Wildenthal<sup>5</sup> and the 2.33 MeV peak with the predicted 2.23 MeV ( $4^+$ ) state. There are no spin assignments in the literature for these two states, but an analogue  $4^+$  state is known at 2.27 MeV in  $^{28}\text{Al}$ . We note that there are several other predicted<sup>5</sup> high-spin states at 2.65 MeV ( $5^+$ ), 3.51 MeV ( $4^+$ ), 4.29 MeV ( $5^+$ ), 4.53 MeV ( $6^+$ ), 5.26 MeV ( $5^+$ ), and higher energies that do not show up prominently in the  $(p, \pi^-)$  spectrum.

We see a weak ground state transition in the  $^{30}\text{Si}(p, \pi^-)^{31}\text{S}$  spectrum shown in Fig. 1(g). This is due to the low spin ( $1/2^+$ ) of the ground state. This peak is well separated from the second excited state peak at 2.24 MeV ( $5/2^+$ ). The first excited state ( $3/2^+$ ) is missing from the spectrum. Our energy calibration scheme gives energies of 0.05 and 2.20 MeV for the ground and 2.24 MeV states, respectively, showing consistency within the measurement error. The 3.19 MeV peak in the spectrum is a doublet corresponding to the known 3.08 ( $1/2^+$ ) and 3.29 ( $5/2^+$ ) MeV states. The 8.33 MeV peak may correspond to one of the known states at 8.18, 8.36, and 8.45 MeV, which have been identified using the  $^{29}\text{Si}(^3\text{He}, n)^{31}\text{S}$  and  $^{29}\text{Si}(^3\text{He}, n\gamma)^{31}\text{S}$  transfer reactions at 6.5 MeV.<sup>7</sup> The strong peaks located near the high excitation energy end of the spectrum are due to the ground state and low lying excited states of

$^{17}\text{Ne}$  resulting from the  $^{16}\text{O}(p, \pi^-)^{17}\text{Ne}$  reaction, which has a much more negative Q-value than the  $^{30}\text{Si}(p, \pi^-)^{31}\text{S}$  reaction. The  $^{30}\text{Si}(p, \pi^-)^{31}\text{S}$  reaction is expected to populate most strongly final states containing a large component of the stretched 2p-1h configuration  $[(\pi d_{3/2})^2 2 (v d_{5/2})^{-1}]_{9/2^+}$ . A  $9/2^+$  state is predicted<sup>5</sup> at 8.31 MeV, which may correspond to the 8.33 MeV peak in the  $(p, \pi^-)$  spectrum; however, we note that thirteen  $9/2^+$  states are predicted in the 5.21 - 9.0 MeV excitation energy region. The 10.58 and 13.33 MeV peaks in the  $(p, \pi^-)$  spectrum may correspond to states outside of the sd-shell model space.

The results and conclusions discussed above are summarized in Table I.

In summary, we have used the  $(p, \pi^-)$  reaction as a spectroscopic tool to identify a number of possible high-spin, two-particle one-hole states in several sd-shell nuclei. Many of these assignments are consistent with recent shell model predictions<sup>5</sup> for the energies of high spin states. More stringent tests of the shell model calculations require knowledge of the matrix elements of the appropriate operators between the states of interest.

<sup>†</sup>Present address: Physics Department, Carnegie-Mellon University, Pittsburgh, PA. 15213.

<sup>§</sup>Present address: Department of Nuclear Energy, Brookhaven National Laboratory, Upton, Long Island, NY. 11973.

- 1) S.E. Vigdor, T.G. Throwe, M.C. Green, W.W. Jacobs, R.D. Bent, J.J. Kehayias, W.K. Pitts, and T.E. Ward, Phys. Rev. Lett. 49, 1314 (1982); Nucl. Phys. A396, 61c (1983).
- 2) W.W. Jacobs, T.G. Throwe, S.E. Vigdor, M.C. Green, J.R. Hall, H.O. Meyer, and W.K. Pitts, Phys. Rev. Lett. 49, 855 (1982).
- 3) J.J. Kehayias, R.D. Bent, M.C. Green, M. Hugi, H. Nann, and T.E. Ward, Phys. Rev. C33, 1388 (1986).
- 4) T.G. Throwe, Ph.D. Thesis, Indiana University, 1985 (unpublished).

Table I. Energies of Levels Strongly Populated in the  $(p, \pi^-)$  Reaction and Inferred Spin Assignments

nucleus	Present Work		Known Levels		nucleus	Present Work		Known Levels	
	$E_x^\dagger$ (MeV)	J	$E_x$ (MeV)	J		$E_x^\dagger$ (MeV)	J	$E_x$ (MeV)	J
$^{20}\text{Na}$	0.74		0.77	$\leq 4^*$	$^{30}\text{S}$	0.00		0.00	0
	1.85		1.92	$\leq 5^*$		2.19		2.21	2
	3.01	6 or 7	2.89			3.49		3.40	2
	4.11	6 or 7	4.33					3.68	$1^*$
$^{24}\text{Al}$	0.03		0.00	4	5.95	4 or 5	5.90		
	1.22		1.12	$2^*$	7.46	4 or 5			
			1.29	$3^*$	9.13	4 or 5			
	3.39		3.35	$2^*$	10.07	4 or 5			
	4.39		4.34						
		4.53							
	5.19	3 - 8							
$^{26}\text{Si}$	-0.17		0.00	0	$^{31}\text{S}$	0.05		0.00	$1/2$
	2.50		2.78	2		2.20		2.24	$5/2$
	7.08	2 - 8	7.15			3.19		3.08	$1/2$
	8.25	2 - 8						3.29	$5/2^*$
	12.00	2 - 8						8.16	
						8.33	$9/2$	8.36	
								8.45	
						10.58	$(9/2)$		
						13.33	$(9/2)$		
$^{28}\text{P}$	-0.04		0.00	3					
			0.11	2					
	1.11		1.13	$3^*$					
	2.32	2 - 7	2.10	$4^*$					
	3.37		3.24						
4.73	2 - 7	4.94							

† Errors  $\approx \pm 0.1$  MeV for all excitation energies determined from the  $(p, \pi^-)$  reaction.

\* The spin and parity of the corresponding isobaric analogue state.

5) B.H. Wildenthal, private communication, 1983.

6) R.A. Paddock, Phys. Rev. C5, 485 (1972).

7) J.M. Davidson, D.A. Hutcheon, D.R. Gill, T. Taylor, D.M. Sheppard, and W.C. Olsen, Nucl. Phys. A240, 253 (1975).